Bioorganic & Medicinal Chemistry, Vol. 1, No. 1, pp. 27-38, 1993
Printed in Great Britain

0968-0896/93 $6.00 + .00

Evaluation of Functional Analogs of CC-1065 and the Duocarmycins Incorporating the Cross-linking 9a-Chloromethyl-1,2,9,9a-tetrahydrocyclopropa[*c*]benz[*e*]indol-4-one (C_2BI) Alkylation Subunit

Dale L. Boger,* Douglas S. Johnson, Moorthy S. S. Palanki,
Department of Chemistry, The Scripps Research Institute, 10666 North Torrey Pines Road, La Jolla, CA 92037

Paul A. Kitos, Jiyoung Chang and Paul Dowell
Department of Biochemistry, University of Kansas, Lawrence, KS 66045

(*Received* 3 *December* 1992)

Abstract–The DNA alkylation properties and *in vitro* cytotoxic activity of a series of analogs of CC-1065 and the duocarmycins incorporating the 9a-chloromethyl-1,2,9,9a-tetrahydrocyclopropa[*c*]benz[*e*]indol-4-one (C_2BI) alkylation subunit are detailed. The C_2BI-based agents have been shown to alkylate DNA within the minor groove in a fashion analogous to CC-1065 or duocarmycin. The stereoelectronically-controlled adenine N3 addition to the least substituted cyclopropane carbon occurs with a selectivity that represents a composite of the two enantiomers of the corresponding CBI-based agents. Additional high affinity alkylation sites were detected which were not prominent alkylation sites for either enantiomer of the CBI-based agents. Such sites may represent induced high affinity alkylation sites resulting from DNA cross-linking following complementary strand alkylation at a high affinity alkylation site and each such site detected proved consistent with predicted models of an adenine–adenine cross-linking event. Further, consistent with this interpretation, the C_2BI agents were shown to constitute efficient cross-linking agents with DNA cross-linking being observed at the same concentrations as DNA alkylation. In comparison to the parent CBI-based agents, the C_2BI-based agents proved to be approximately 100–10,000x less effective at DNA alkylation and 100–10,000x less potent in cytotoxic assays. This is suggested to be the consequence of a significant steric deceleration of the adenine N3 alkylation reaction attributable to the additional 9a-chloromethyl substituent. Consistent with this interpretation, the noncovalent binding constant of C_2BI–$CDPI_2$ for poly[dA]–poly[dT] proved nearly identical to that of $CDPI_3$ under kinetic binding conditions, and prolonged incubation of C_2BI–$CDPI_2$ with poly[dA]–poly[dT] (72 h, 25°C) provided covalent complexes with a helix stabilization comparable to that observed with (+)- or (–)-CPI–$CDPI_2$ indicating that the size of the C_2BI subunit inhibits but does not preclude productive DNA alkylation.

(+)-CC- 1065 (**1**)[1–8] and (+)-duocarmycin A (**2**)[9–13] constitute the initial members of a growing class of potent, naturally occurring antitumor antibiotics that derive their biological properties through sequence-selective DNA minor groove alkylation, Figure 1. For the natural enantiomers, the stereoelectronically-controlled adenine N3 addition to the unsubstituted cyclopropane carbon of the agent left-hand subunit has been shown to occur within selected AT-rich regions of duplex DNA with a binding orientation that extends in the 3' to 5' direction from the site of alkylation. Some unnatural enantiomers including *ent*-(–)-CC-1065 and closely related agents[14–17] similarly alkylate adenine N3 within selected AT-rich minor groove regions but with a binding orientation that extends in the 5' to 3' direction from the site of alkylation. In recent efforts, we have detailed the preparation of agents incorporating deep-seated changes in the alkylation subunit with the intent of determining the fundamental structural features contributing to polynucleotide recognition and functional reactivity.[18–20] The initial studies in which the CPI-, CI- and CBI-based agents were examined[21–23] have proven useful and agents incorporating the simplified and chemically more stable CBI alkylation subunit have proven especially interesting. Such agents have displayed more potent cytotoxic activity[19] than the corresponding CPI-based agents and selected agents within the CBI series have displayed efficacious antitumor activity.[20] Despite the decreased solvolytic reactivity of the CBI-based agents, they have been found to participate in the characteristic DNA alkylation at a greater rate and with a higher intensity (efficiency) than the corresponding agents possessing the authentic CPI alkylation subunit.[22]

Recently, we have detailed the extension of the studies to the preparation of agents incorporating the 9a-chloromethyl-1,2,9,9a-tetrahydrocyclopropa[*c*]benz[*e*]-indol-4-one (C_2BI) alkylation subunit.[24] Herein we report the results of our evaluation of the C_2BI-based agents **3**–**17**, Figure 2.

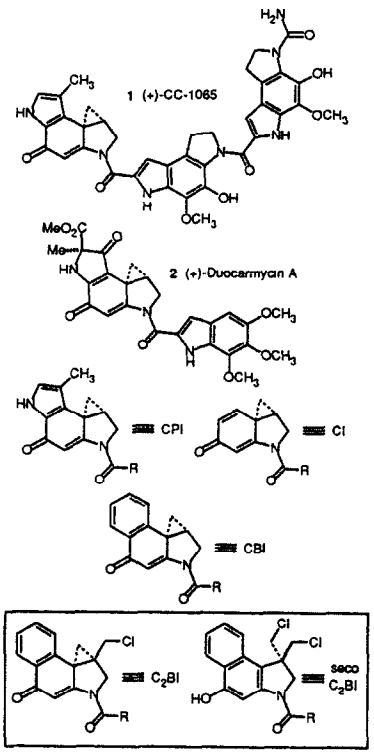

Figure 1.

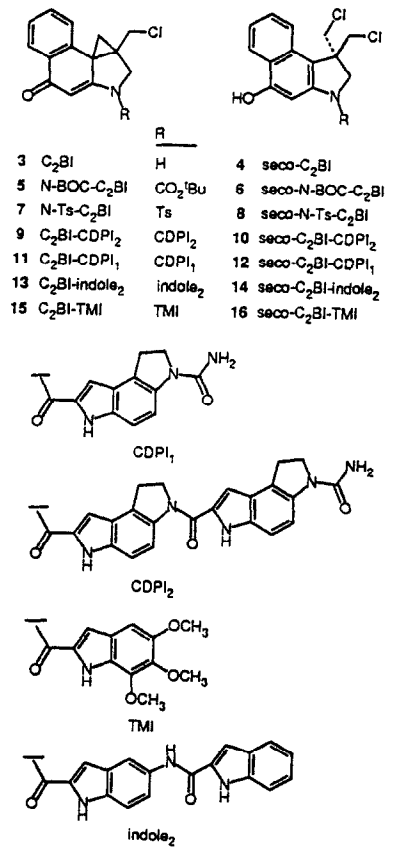

Figure 2.

Design and selection of C_2BI

The selection of C_2BI for synthesis and evaluation was based on the observations that the parent CBI-based agents have proven chemically more stable, biologically more potent, and synthetically more accessible than the corresponding CPI-based agents incorporating the authentic CC-1065 alkylation subunit. Further, the precursor acyclic or *seco*-C_2BI agents, like the *seco*-CBI agents, could be anticipated to display properties comparable to the cyclopropane containing agents but are inherently achiral. Consequently, they provided attractive analog candidates free of the technical considerations of resolution or asymmetric synthesis. Since both (+)-CC-1065 and *ent*-(-)-CC-1065 display efficient DNA alkylation properties and potent biological activity, the potential *in vivo* closure of the achiral *seco*-C_2BI agents to both enantiomers of C_2BI may prove inconsequential if both enantiomers display useful properties. More importantly, the bis-alkylation capabilities of the C_2BI-based agents or their *seco* precursors were anticipated to provide the opportunity for DNA cross-linking, Scheme I. That such a cross-linking event may be reasonable was established in modeling studies of the (+)-CC-1065 (natural enantiomer) high affinity alkylation site within w794 DNA,[25,26] 5'-d(AATTA), which provides the potential for an adenine–adenine cross-link with the additional (unnatural enantiomer) alkylation occurring on the complementary strand one base-pair removed in the 5' direction from the initial alkylation site. Illustrated in Figure 3 is a model of the adenine–adenine cross-link which appears to be capable of being formed with no significant distortion to the model duplex DNA.

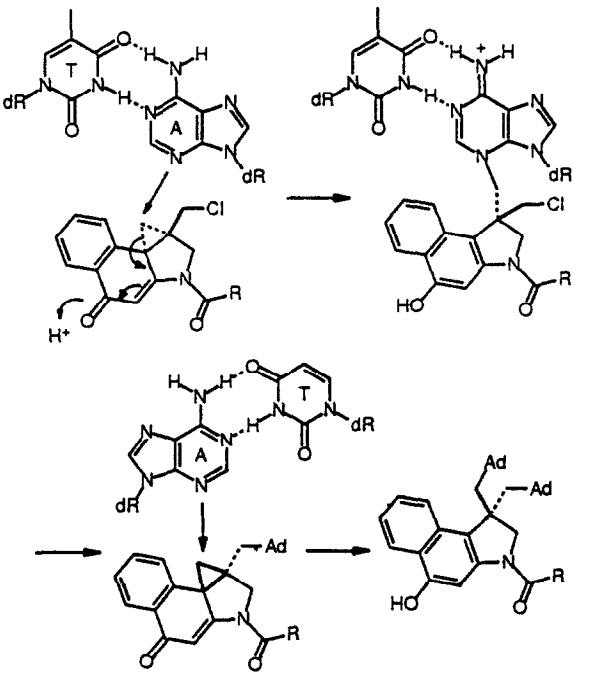

Scheme I.

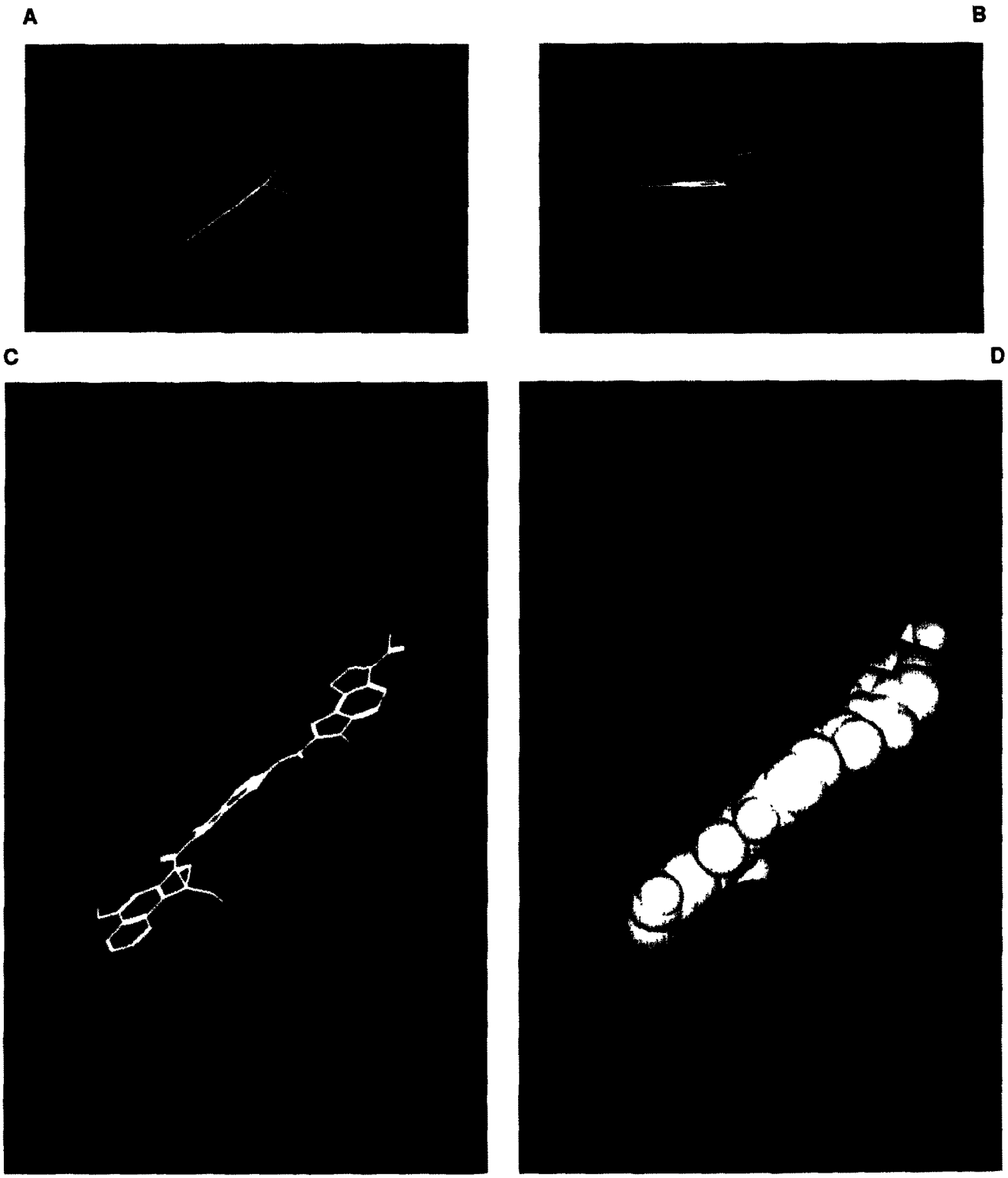

Figure 3 Front and groove views of the C_2BI–$CDPI_2$ cross-linking at the w794 high affinity site. A: Front view of cross-linked d(TTAG)-C_2BI taken from 5'-d(CTCAATTAGTC)–C_2BI–$CDPI_2$. B: Groove view of cross-linked 5'-d(TTAG)–C_2BI. C and D: Stick and space filling model of 5'-d(CTCAATTAGTC)–C_2BI–$CDPI_2$.

DNA binding affinity

In preceding studies, the absolute binding constants of agents related to CC-1065 which cannot participate in a DNA alkylation reaction have been measured.[27–29] The accurate quantification of the noncovalent binding affinity of the agents including $CDPI_n$ (n = 1–5) was established through measurement of the decrease in fluorescence accompanying the displacement of prebound ethidium bromide from DNA.[30] Under the conditions employed, the agents do not interfere with the fluorescence measurements and the noncovalent binding agents related to CC-1065 have been shown to follow a noncompetitive model for binding and ethidium bromide displacement. This was first recognized in studies with $CDPI_3$ (r = 0.2)[27] upon examination of the *linear* plots of % fluorescence versus r ($[agent]_t/[base\text{-}pair]_t$) in which the X-intercept was found to correspond to the ideal [agent]/[base-pair] ratio of 0.2 expected for a minor groove binding site size of five base-pairs. These observations have proven general for a wide range of noncovalent binding agents related to CC-1065.[29] Thus, the noncompetitive and linear displacement of prebound ethidium bromide proceeds in a manner that permits the accurate quantification of DNA bound agent and the measurement of the absolute binding constants according to eq. 1 at 50% fluorescence.[29]

$$K_b = \frac{1}{[agent]_t - 0.5r[base\text{-}pair]_t} \quad (1)$$

r = agent/base-pair binding site size

In our preliminary studies, C_2BI–$CDPI_2$ was observed to only slowly alkylate DNA at a rate which suggested that the noncovalent DNA binding affinity of the agent may be measured without competitive DNA alkylation occurring under the conditions and time frame of the binding constant measurements. Titration of ethidium bromide prebound poly[dA]–poly[dT] with C_2BI–$CDPI_2$ under the conditions previously disclosed[31] provided a linear plot of % fluorescence versus r, Figure 4. The absolute noncovalent binding constant for C_2BI–$CDPI_2$ was determined to be 2.5 x 10^7 M^{-1}, $\Delta G°$ (298 K) = -10.0 kcal/mol, and the X-intercept (r = 0.33) provided a binding site size of three base-pairs. This binding site size of C_2BI–$CDPI_2$ proved nearly identical to that of $CDPI_2$ (K_b = 3.2 x 10^5 M^{-1}, $\Delta G°$ (298 K) = -7.5 kcal/mol, r = 0.3) and the agent affinity nearly identical to that of $CDPI_3$ (K_b = 1.8 x 10^7 M^{-1}, $\Delta G°$ (298 K) = -9.9 kcal/mol, r = 0.2), Table 1. On the basis of additional studies detailed herein, we have interpreted this behavior to represent kinetic DNA minor groove binding of the agent in a manner comparable to that of $CDPI_2$ or $CDPI_3$.

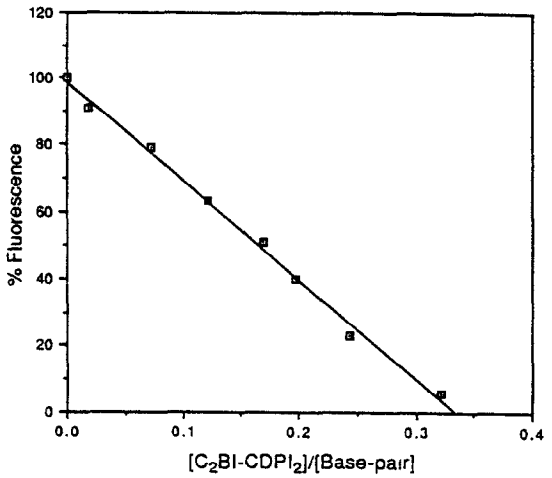

Figure 4 Plot of % fluorescence versus r ($[C_2BI\text{–}CDPI_2]/[base\text{-}pair]$) in the binding constant titration of poly[dA]–poly[dT] (0.79841×10^{-5} M) prebound with ethidium bromide (0.39921×10^{-5} M) with C_2BI–$CDPI_2$ delivered in 0.3 mM DMSO. The buffer solution was 0.1 M Tris-HCl, 0.1 M NaCl, pH = 8.0.

Table 1.

Agent	ΔT_m[a]	K_b[b]	base-pair[c]
$CDPI_2$	0-2°C	3.2 x 10^5 M^{-1}	3.3
$CDPI_3$	13°C	1.8 x 10^7 M^{-1}	5.0
C_2BI-$CDPI_2$	22°C[d]	2.5 x 10^7 M^{-1}	3.0
(+)-CPI-$CDPI_2$	25°C[e]	---	---
(-)-CPI-$CDPI_2$	20°C[e]	---	---

[a] ΔT_m relative to poly[dA]–poly[dT], T_m = 53°C. The DNA hyperchromicity at 260 nm was monitored as a function of temperature with 1:10 agent:base-pair ratio (alkylating agents) or 1:7 agent:base-pair ratio ($CDPI_2$, $CDPI_3$) incubated at 25°C, 3 days in 10 mM phosphate buffer (pH = 7.2) with 0.3% DMSO.
[b] Binding constant (K_b) for poly[dA]–poly[dT] determined as described.
[c] Base-pair binding site size of agent determined in K_b measurement.
[d] Conducted with *seco*-C_2BI–$CDPI_2$ (**10**).
[e] Taken from Ref. 15.

DNA–agent complex thermal denaturation studies

The DNA binding of the agents was further confirmed in studies of the stabilization of the thermally-induced helix to coil melting transition of poly[dA]–poly[dT], Table 1. In contrast to the binding constant measurement studies, the studies were conducted after DNA–agent incubation at 25°C for 72 h and they revealed that C_2BI–$CDPI_2$ bound to DNA in a manner which provided a helix stabilization comparable to that of (+)-CPI-$CDPI_2$ or (-)-CPI–$CDPI_2$ and that this substantially exceeded that of $CDPI_2$ or $CDPI_3$. This provided conclusive evidence that the agent was bound to DNA in a covalent rather than noncovalent manner under the thermodynamic binding conditions and that full agent binding in the minor groove is accessible. It also suggests that after the 3 day

incubation at 25°C either the extent of DNA alkylation and helix stabilization for C_2BI–$CDPI_2$ was equivalent to that of (+)- and (–)-CPI–$CDPI_2$ or that the extent of alkylation was less than that of (+)- and (–)-CPI–$CDPI_2$ but the stabilization derived from the alkylation was proportionally enhanced through cross-linking. As a consequence of the studies detailed in the following two sections, the latter explanation for the observations appears most likely.

DNA alkylation: intensity and selectivity

The examination of the DNA alkylation properties of C_2BI–$CDPI_2$ (**9**) within duplex w794 DNA and its complement w836 DNA[25] for which comparison results are available for related agents[15,20–23] was conducted in efforts to demonstrate the event and selectivity of DNA alkylation and the DNA cross-linking capabilities. The demonstration of DNA alkylation and the identification of the adenine N3 alkylation sites were obtained from the thermally-induced strand cleavage of singly ^{32}P 5'-end-labeled double stranded DNA after exposure to the agents following past protocols.[26] Thus, incubation of **9** and its *seco* precursor **10** with the labeled duplex DNA (25°C and 37°C, 24–96 h), removal of the unbound agent by EtOH precipitation of the DNA, resuspension of the alkylated DNA in aqueous buffer, thermal treatment (100°C, 30 min) to induce strand cleavage at the adenine N3 alkylation sites, and electrophoresis of the resultant DNA adjacent to Sanger sequencing standards[32] under denaturing conditions followed by autoradiography permitted identification of the adenine N3 sites of DNA alkylation, Figures 5–7. The *seco* agent **10** proved to be approximately 10–100x more effective than C_2BI–$CDPI_2$ at alkylating DNA under the conditions of the examination and the two agents exhibited an identical DNA alkylation selectivity. Moreover, the selectivity of the DNA alkylation appears to represent a composite of the readily distinguishable alkylation profiles of (+)-CBI–$CDPI_2$ and (–)-CBI–$CDPI_2$. For example, the w794 high affinity alkylation site for (+)-CBI–$CDPI_2$ is the single site 1 (5'-AATTA) and that of (–)-CBI–$CDPI_2$ is primarily the single site 2 (5'-ATTTT) with little or no crossover alkylation between these two sites.[22] In contrast, both sites constitute nearly equivalent high affinity alkylation sites for **9** and **10** and both sites provide the opportunity for the adenine–adenine cross-linking detailed in Scheme I and illustrated in Figure 3.[33] Similarly, the remaining two sites labeled in Figure 5 constitute low affinity alkylation sites for (+)-CBI–$CDPI_2$ and are not readily alkylated by (–)-CBI–$CDPI_2$. However, the complementary strand contains high affinity alkylation sites for (–)-CBI–$CDPI_2$ adjacent to these sites one base pair removed in the 5' direction. It is likely that alkylation at the complementary strand high affinity alkylation sites leads to cross-linking with induced high affinity alkylation at these two sites as illustrated in Figure 3. Within w794 DNA, the *seco* agent **10** proved to alkylate the DNA at concentrations approximately 100x lower than that required for **9** and at concentrations approximately 10^4–10^5 higher than that required of (+)- and (–)-CBI–$CDPI_2$.

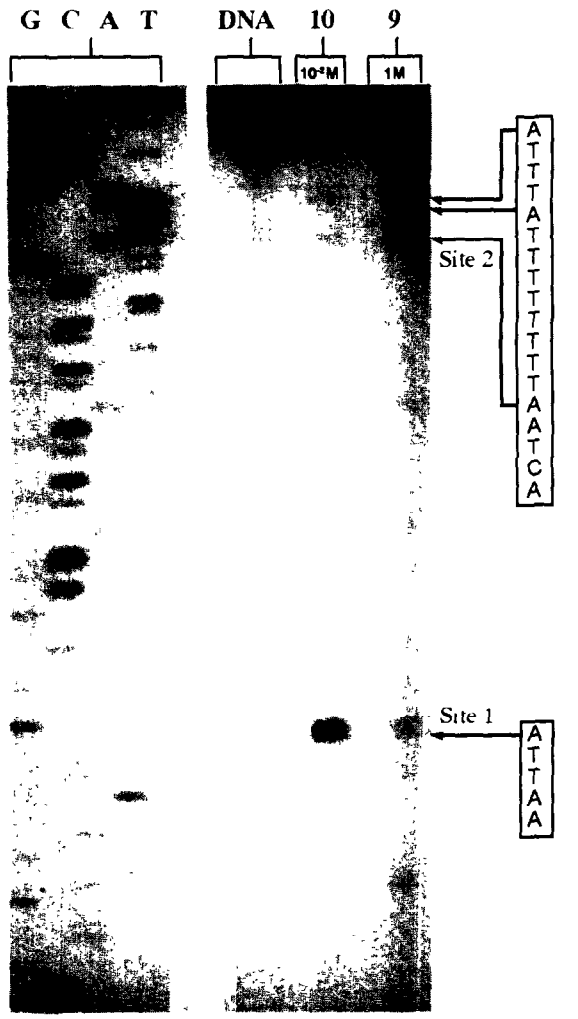

Figure 5 Thermally-induced strand cleavage of w794 duplex DNA (SV40 DNA segment, 144 b.p., nucleotide no. 138-5238). DNA–agent incubation at 37°C, removal of unbound agent and 30 min thermolysis (100°C) followed by denaturing 8% PAGE and autoradiography. Lanes 1–4, Sanger G, C, A, and T reactions; lane 5, control DNA; lane 6, 0.01 M **10**; lane 7, 1 M **9**. The observation and origin of double bands for a single alkylation site (i.e., site 1) have been discussed in detail elsewhere, Ref. 26.

This evaluation is not to say that the profile of DNA alkylation by C_2BI–$CDPI_2$ must resemble that exhibited by (+)-CBI–$CDPI_2$ and/or (–)-CBI–$CDPI_2$ as it does within w794 DNA. In sharp contrast, the w836 DNA alkylation profile of C_2BI–$CDPI_2$ proved to be much different than that of (+)- or (–)-CBI–$CDPI_2$, Figure 6. A single high affinity site for C_2BI–$CDPI_2$ (5'AATA) was observed which constitutes only a low affinity site for (+)-CBI–$CDPI_2$ and a site not alkylated by (–)-CBI–$CDPI_2$. In part, the observation of this single high affinity alkylation site for C_2BI–$CDPI_2$ (5'-AATA) may be attributed to an adenine–adenine cross-linking reaction with induced high affinity alkylation resulting from a

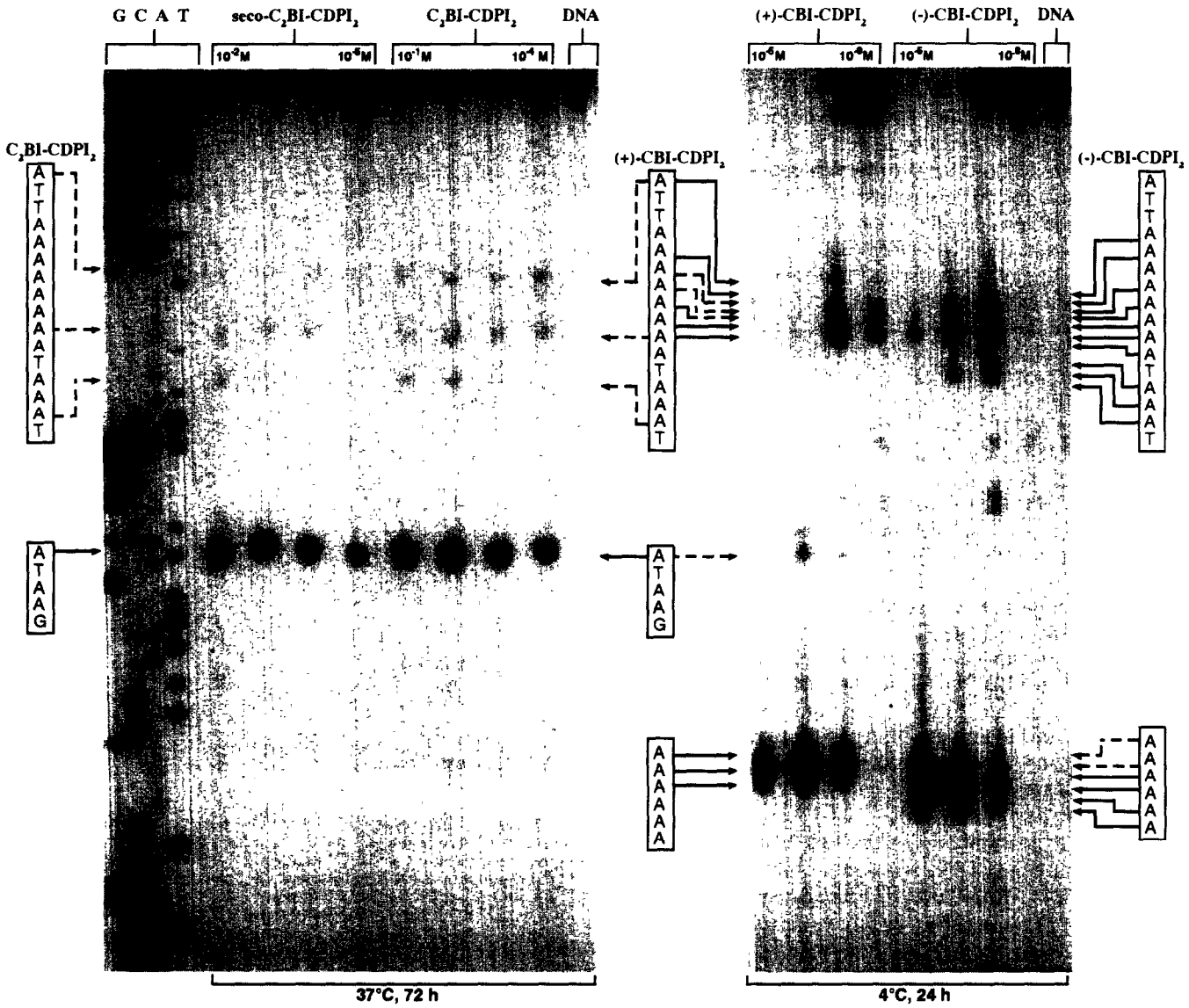

Figure 6 Thermally-induced strand cleavage of w836 duplex DNA (SV40 DNA segment, 146 b.p., nucleotide no. 5189-91). DNA–agent incubation at 4°C or 37°C (24–72 h), removal of unbound agent and 30 min thermolysis (100°C) followed by denaturing 8% PAGE and autoradiography. Lanes 1–4, Sanger G, C, A, T reactions; lanes 5–8, *seco*-C_2BI–$CDPI_2$ (**10**, 1 x 10^{-2} – 1 x 10^{-5} M; 37°C, 72 h); lanes 9–12, C_2BI–$CDPI_2$ (**9**, 1 x 10^{-1} – 1 x 10^{-4} M; 37°C, 72 h); lane 13, control DNA (37°C, 72 h); lanes 14–17, (+)-CBI–$CDPI_2$ (1 x 10^{-5} – 1 x 10^{-8} M; 4°C, 24 h); lanes 18–21, (–)-CBI–$CDPI_2$ (1 x 10^{-5} – 1 x 10^{-8} M; 4°C, 24 h); lane 22, control DNA (4°C, 24 h).

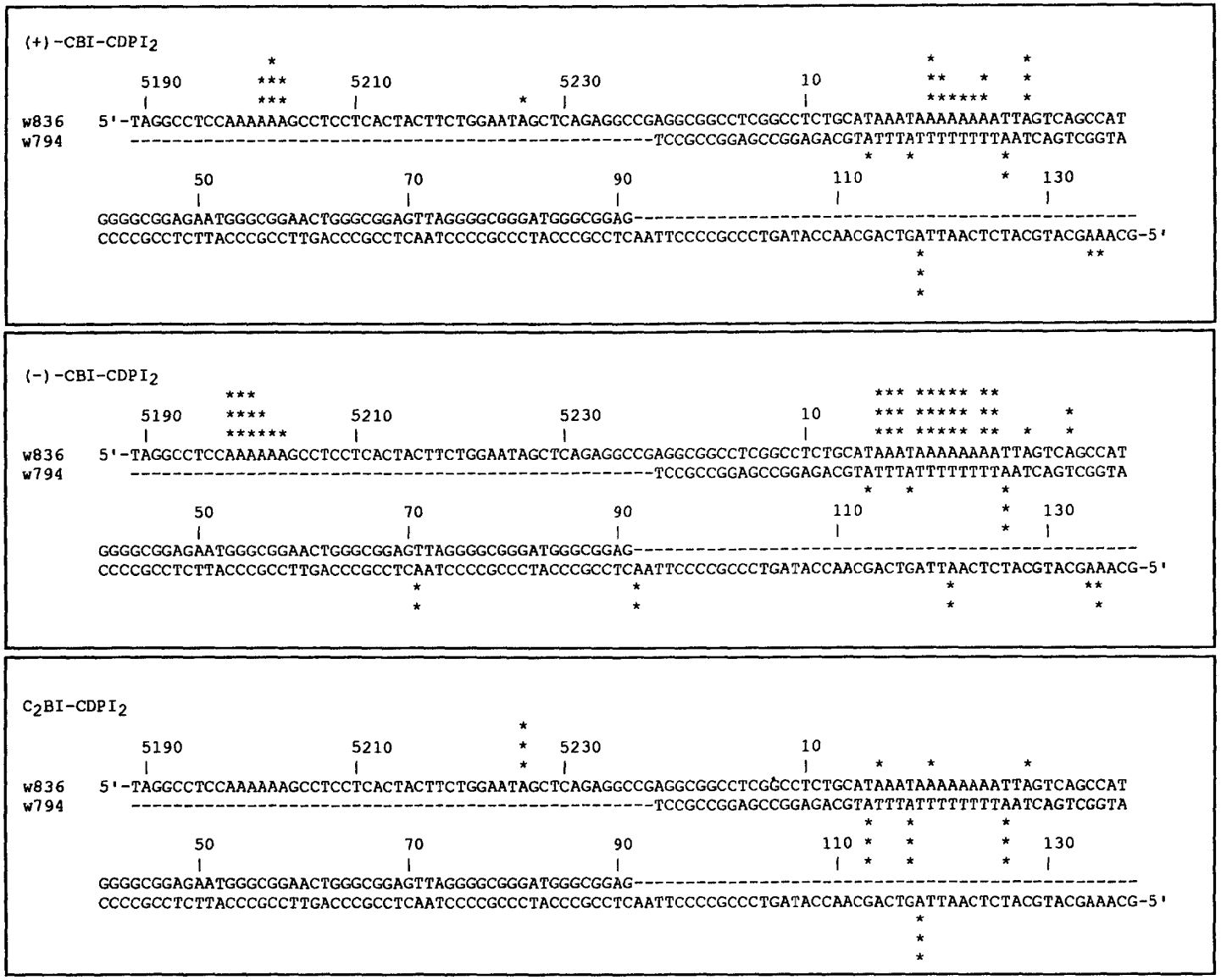

Figure 7 Summary of alkylation sites for (+)-CBI–$CDPI_2$, (–)-CBI–$CDPI_2$, and C_2BI–$CDPI_2$ within w794 and w836 DNA. The relative intensity of alkylation (thermal cleavage) at each site is indicated with the number of symbols above a given site: *** (high affinity), ** (medium affinity), * (low affinity). The SV40 nucleotide numbering system uses the replication origin (ORI) as reference. The missing terminal regions of the DNA represented by a line constitute the overlapping regions not present on the complementary clones available for examination and is not a single-stranded segment of DNA.

dominant high affinity alkylation site on the complementary strand (5'-TTAT) for the unnatural enantiomers. Within w836, the *seco* agent **10** proved to alkylate the DNA at concentrations approximately 1–10x lower than that required for **9** and at concentrations approximately 100–1000x higher than that required of (+)- and (–)- CBI–$CDPI_2$. Figure 7 summarizes the comparative DNA alkylation sites of C_2BI–$CDPI_2$, (+) and (–)-CBI–$CDPI_2$ within w794 and w836 DNA.

A brief comparative examination of the DNA alkylation properties of **5–6** and **9–16** was conducted within w794 and w836 DNA. Only a rather nonselective and poorly defined alkylation of DNA by **5** and **17** was detected at high agent concentrations (1 M, 37°C, 72 h) and a slightly more effective but still weak and nondiscriminant DNA alkylation was observed with the *seco* derivative **6** (10^{-1} M). With the advanced analogs, the relative efficiency of w794 alkylation (37°C, 48 h) observed was pronounced with C_2BI–$CDPI_2$ (alkylation at 10^{-3}–10^{-4} M) > C_2BI–$CDPI_1$ (10^{-2} M but weak) > C_2BI–$indole_2$, C_2BI–TMI (no alkylation at 10^{-2} M). Moreover, both the rate and intensity of DNA alkylation by C_2BI–$CDPI_2$ or *seco*-C_2BI–$CDPI_2$ proved to be substantially lower than that of (+)- or (–)-CBI–$CDPI_2$ as judged by the concentration of agent and reaction conditions required for observation of DNA alkylation. (+)-CBI–$CDPI_2$ (rel. efficiency = 1) was disclosed earlier[22] to be slightly more, effective than the unnatural enantiomer (–)-CBI–$CDPI_2$ (0.5–0.1x) and both agents alkylate w794 at 4°C, 24 h at 10^{-6}–10^{-8} M agent concentrations. Both agents proved to be substantially more effective than **9** or **10** which alkylate w794 only at higher agent concentrations (10^{-3}–10^{-4} M) and only under more vigorous reaction conditions (37°C, 24–96 h). Similarly, the relative efficiency of w836 DNA alkylation observed was: (+)-CBI–$CDPI_2$ (alkylation at 10^{-7}–10^{-8} M; 4°C, 24 h) > (–)-CBI–$CDPI_2$ (10^{-6}–10^{-7} M; 4°C, 24 h) > *seco*-C_2BI–$CDPI_2$ (10^{-5}–10^{-6} M; 37°C, 72 h) > C_2BI–$CDPI_2$ (10^{-4}–10^{-5} M) > *seco*-C_2BI–$CDPI_1$ (10^{-3}–10^{-2} M) ≥ *seco*-C_2BI–$indole_2$ (10^{-2} M but weak) ≥ *seco*-C_2BI–TMI (10^{-3}–10^{-1} M but weak).[34] Thus, within the series of C_2BI-based agents examined, the effectiveness of the DNA alkylation diminished as the size and DNA binding capabilities of the agent were reduced.

In efforts to ensure that the properties of the agents may not be significantly altered or diminished by the selection of the 9a-methyl substituent, the mesylate derivative **17** of N-BOC–C_2BI was prepared for direct comparison with the chloro derivative **5** of N-BOC–C_2BI. In the comparison limited to the examination of **5** versus **17**, the relative size and reactivity of the 9a-methyl substituent did not appear to significantly alter the observed DNA alkylation selectivity or efficiency and both agents behaved in a comparable manner. Although the reduced C_2BI alkylation capabilities could be related to the unusually stable ring system which is approximately 12x more stable than the CBI nucleus toward solvolysis or alkylation,[24] it most likely may be attributed to the steric inhibition of the requisite adenine N3 alkylation. This in turn may be due to steric inhibition of the noncovalent binding within the minor groove preceding alkylation, steric deceleration of the bound agent alkylation step itself, or competitive alkylation reactivity toward unidentified sites diminishing the effective concentration at which adenine N3 alkylation is observed. As revealed in the binding constant measurements, this most likely may be attributed to steric inhibition of the bound agent adenine N3 alkylation reaction.

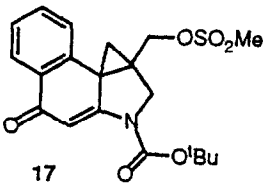

17

DNA alkylation: cross-linking

The DNA cross-linking[35] properties of *seco*-C_2BI–$CDPI_2$ (**10**) were examined within w794 duplex DNA under conditions which permit the results to be compared with those of the w794 strand cleavage assay detailed above. Using this protocol, the studies were anticipated to provide a qualitative assessment of the relative efficiency of cross-linking versus DNA monoalkylation. Thus, treatment of the singly 5' end-labeled w794 DNA with **10** (37°C, 24 h) was conducted as detailed above with the exception that the alkylated DNA was not subjected to the thermal strand cleavage reaction conditions. Gel electrophoresis of the resultant DNA under denaturing conditions followed by autoradiography provided two bands, one of which proved to be the cross-linked DNA, Figure 8. The faster moving lower molecular weight band constitutes the unmodified or alkylated but noncross-linked single-stranded labeled DNA and the slower moving band constitutes the cross-linked duplex DNA (template-labeled DNA cross-link). The agent **10** exhibited detectable DNA cross-linking at 10^{-3} M, which was the lowest concentration at which DNA alkylation was detected with DNA–agent incubation conducted at 37°C, 24 h, exhibited 20% cross-linking at 10^{-2} M which was a concentration at which 35% DNA alkylation was observed, and exhibited nearly complete (98%) cross-linking of the duplex DNA at 10^{-1} M, the concentration at which approximately 80–100% of the labeled DNA was alkylated. Thus, the cross-linking by **10** was observed at concentrations essentially identical to that required for DNA alkylation verifying a high cross-linking efficiency.

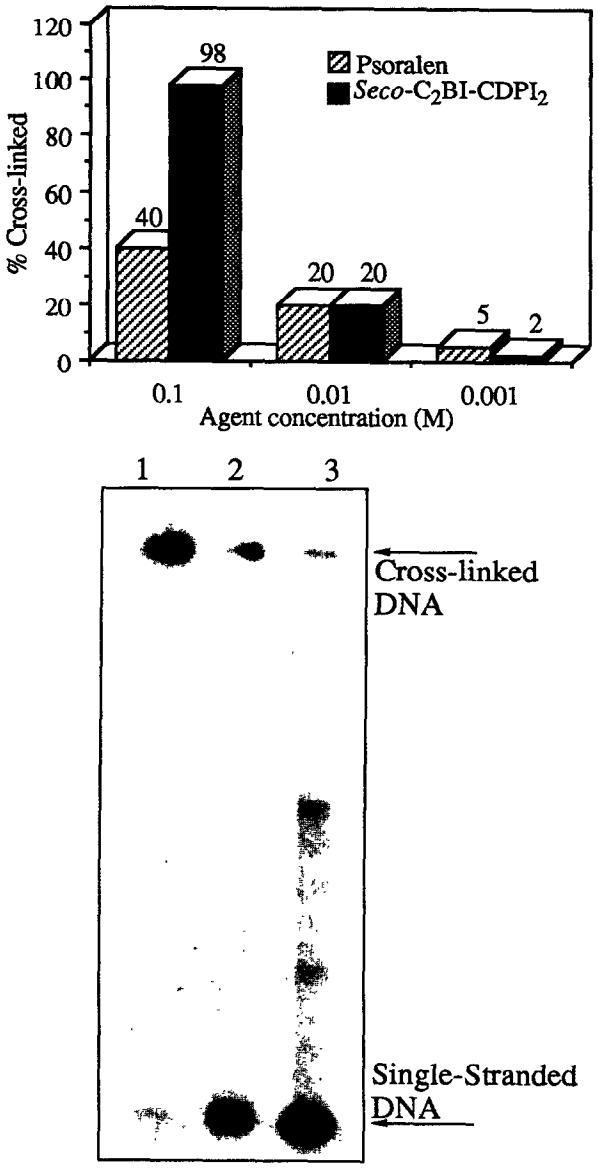

Figure 8 Cross-linking study of *seco*-C_2BI–$CDPI_2$ (**10**) with w794 duplex DNA. DNA–agent incubation at 37°C (24 h, pH 6), removal of unbound agent followed by denaturing 8% PAGE and autoradiography. Lanes 1–3, 0.1, 0.01, and 0.001 M **10**. Quantification of the extent of cross-linking was conducted using a Millipore Bio Image 60S RFLP system and run adjacent to psoralen (hυ 365 nm, 1 h) as a positive cross-linking control (data not shown).

In vitro *cytotoxic activity*

The results of the *in vitro* cytotoxic evaluation of the C_2BI-based agents are summarized in Table 2.[36] Consistent with their relative intensity of DNA alkylation, the C_2BI-based agents proved to be considerably less potent than the parent CBI-based agents or agents incorporating the authentic CPI alkylation subunit. The most potent of the agents examined proved to be C_2BI–$CDPI_2$ which was found to be approximately 1000x less potent than (+)-CC-1065 or the natural enantiomer of CBI–$CDPI_2$ or CPI–$CDPI_2$ and, correspondingly, approximately 1000x less effective at DNA alkylation. Unlike the CBI- and CPI-based agents but consistent with their trends in DNA alkylation intensity, the additional C_2BI analogs including C_2BI–$CDPI_1$, C_2BI–indole$_2$, and C_2BI–TMI proved to be less potent than C_2BI–$CDPI_2$ and approximately 10,000x less potent than analogous CBI- or CPI-based agents. The distinctions were less pronounced with the simple derivatives of C_2BI including N-BOC–C_2BI and *N*-Ts–C_2BI which proved to be 5–100x less potent than the corresponding CBI- or CPI-based agent. In addition, in the limited comparison of **5** and **17** the relative size and reactivity of the 9a-methyl substituent did not significantly alter the relative cytotoxic potency of the agents. Within the full series of C_2BI agents, the cytotoxic potency was found to decrease as the size and DNA binding capabilities of the agent were decreased. Consequently, the extent of the noncovalent DNA binding of the agents appears to significantly effect the biological potency of the C_2BI agents. This contrasts the observations made with the natural enantiomers of the CBI or CPI-based agents in which the simple event,[15] not extent, of noncovalent DNA binding seems responsible for observation of potent cytotoxic activity.

Table 2. *In vitro* cytotoxic activity, L1210

Agent		IC_{50} (nM)
3	C_2BI	33000
5	*N*-BOC-C_2BI	12000
6		8000
17		8000
7	*N*-Ts-C_2BI	5000
8		12000
9	C_2BI-$CDPI_2$	6
10		3
11	C_2BI-$CDPI_1$	6300
12		700
13	C_2BI-indole$_2$	900
14		700
15	C_2BI-TMI	---
16		5000
(+)-CBI		7000
(+)-*N*-BOC-CBI		80
(-)-*N*-BOC-CBI		900
(+)-CBI-$CDPI_2$		0.005
(-)-CBI-$CDPI_2$		0.04
(+)-CBI-$CDPI_1$		0.005
(-)-CBI-$CDPI_1$		≥ 0.4
(+)-CBI-indole$_2$		0.01
(+)-*N*-BOC-CPI		300
(+)-CPI-$CDPI_2$		0.02
(-)-CPI-$CDPI_2$		0.02
(+)-CPI-$CDPI_1$		0.04
(-)-CPI-$CDPI_1$		≥ 6
(+)-CPI-indole$_2$		0.04
(+)-CC-1065		0.02
(-)-CC-1065		0.02

Conclusions

The C_2BI-based agents have been shown to alkylate DNA within the minor groove in a fashion analogous to CC-1065 or duocarmycin. The stereoelectronically-controlled adenine N3 addition to the least substituted cyclopropane carbon occurs with a selectivity that represents a composite of the two enantiomers of the corresponding CBI-based agents. Additional high affinity alkylation sites were detected that are not prominent alkylation sites for either enantiomer of the CBI-based agents. Such sites may represent induced high affinity alkylation sites resulting from DNA cross-linking following complementary strand alkylation at a high affinity alkylation site and each such site detected proved consistent with predicted models of an adenine–adenine cross-linking event. Further, consistent with this interpretation, the C_2BI agents were shown to constitute efficient DNA cross-linking agents with cross-linking being observed at the same concentrations that DNA alkylation was detected.

In comparison with the parent CBI-based agents, the C_2BI-based agents proved to be approximately 100–10,000x less effective at DNA alkylation and 100–10,000x less potent in cytotoxic assays. This is suggested to be the consequence of a significant steric deceleration of the adenine N3 alkylation reaction attributable to the additional 9a-chloromethyl substituent of the agent. Consistent with this interpretation, the noncovalent binding constant of C_2BI–$CDPI_2$ for poly[dA]–poly[dT] proved nearly identical to that of $CDPI_3$ under kinetic binding conditions and prolonged incubation of C_2BI–$CDPI_2$ with poly[dA]–poly[dT] (72 h, 25°C) provided covalent complexes with a helix stabilization comparable to that observed with (+)- or (–)-CPI–$CDPI_2$ indicating that the size of the C_2BI subunit inhibits but does not preclude productive DNA alkylation.

Experimental

Proton and carbon nuclear magnetic resonance spectra (^1H NMR and ^{13}C NMR) were obtained on a Bruker AM 400 spectrometer. Infrared spectra (IR) were recorded on a Perkin–Elmer IR 1600. Preparative centrifugal thin-layer chromatography (PCTLC) was performed on a Harrison Model 7924 Chromatotron (Harrison Research, Palo Alto, CA) using Merck silica gel 60 PF_{254} containing $CaSO_4$–$0.5H_2O$ binder. UV spectra were recorded on a Varian Cary 4 UV-Visible spectrophotometer. General procedures, the preparation of singly ^{32}P 5'-end-labeled double-stranded DNA, the agent binding studies, gel electrophoresis, and autoradiography were conducted following protocols described in full detail[26] and the preparation of agents **3–16** have been detailed elsewhere.[24] Fluorescence measurements used in the DNA binding studies were obtained on a SLM Aminco Bowman Series 2 Luminescence Spectrometer. The DNA (poly[dA]–poly[dT]) used in the binding constant and thermal denaturation studies was purchased from Sigma. The DNA hyperchromicity versus temperature was measured on a Varian Cary 4 UV-Visible Spectrophotometer equipped with a water circulating bath.

N-(tert-*Butyloxycarbonyl)-9a-(methanesulfonyloxy-methyl)-1,2,9,9a-tetrahydrocyclopropa[c]benz[[e]indol-4-one (17)*

A solution of 1,1-bis(hydroxymethyl)-3-(*tert*-butyloxycarbonyl)-5-hydroxy-1,2-dihydro-3*H*-benz[*e*]indole [24] (8.0 mg, 23 μmol), methanesulfonic anhydride (8.9 mg, 51 μmol, 2.2 equiv.), pyridine (4.1 μL, 51 μmol, 2.2 equiv.) in EtOAc (250 μL) and CH_2Cl_2 (250 μL) was stirred at 23°C for 2 h. PCTLC (1 mm SiO_2, 33% EtOAc–hexane) afforded 1,1-bis(methanesulfonyloxy)-3-(*tert*-butyloxycarbonyl)-5-hydroxy-1,2-dihydro-3*H*-benz[*e*]-indole (**18**, 5.9 mg, 51%) and **17** (1.7 mg, 18%). Compound **18** was unstable and immediately converted to **17**. A solution of **18** (2 mg, 4 μmol), NaH (60%, 0.5 mg, 12 μmol, 3 equiv) in THF (0.5 mL) was stirred at 23°C for 1 h. The reaction mixture was filtered through a SiO_2 plug which was washed with EtOAc (3 x 1 mL). The filtrate was combined and concentrated *in vacuo*. PCTLC (1 mm x 5 cm SiO_2, 33% EtOAc–hexane) afforded **17** (1.3 mg, 81%) as a thick oil: ^1H NMR ($CDCl_3$, 400 MHz) δ 8.31 (d, 1H, J = 8 Hz, C5-H), 7.54 (t, 1H, J = 8 Hz, C7-H), 7.45 (t, 1H, J = 8 Hz, C6-H), 7.09 (d, 1H, J = 8 Hz, C8-H), 6.92 (bs, 1H, C3-H), 5.04 and 4.76 (two d, 2H, J = 12 Hz, CH_2OMs), 4.12 and 3.97 (two d, 2H, J = 11 Hz, C1-H), 3.00 (s, 3H, CH_3), 1.97 (d, 1H, J = 5 Hz, C9-H), 1.80 (d, 1H, J = 5 Hz, C9-H), 1.57 (s, 9H, $C(CH_3)_3$); ^{13}C NMR ($CDCl_3$, 50 MHz) δ 184.7, 137.4, 133.0, 131.2, 127.7, 127.1, 121.8, 109.6, 77.2, 66.9, 56.3, 38.1, 37.5, 36.1, 34.8, 31.9, 29.7, 28.2; IR (solid film) υ_{max} 2983, 1739, 1629, 1413, 1321, 1151, 1036, 857 cm^{-1}; FABMS (NBA–CsI), m/e 538 ($M + Cs^+$, 100); FABHRMS m/e 538.0305 ($C_{20}H_{23}NO_6S + Cs^+$ requires 538.0300).

DNA binding constant studies

A solution of poly[dA]–poly[dT] (0.79841×10^{-5} M) and ethidium bromide (0.39921×10^{-5} M) was prepared to provide a 2:1 ratio of base-pair:ethidium bromide in a 0.1 M Tris-HCl, 0.1 M NaCl, pH = 8.0 buffer solution. The fluorescence spectrophotometer was calibrated at 23°C to 100% F and 0% F with the DNA–ethidium bromide buffer solution and an equivalent ethidium bromide buffer solution, respectively. The premixed DNA–ethidium bromide solution was titrated dropwise with a solution of C_2BI–$CDPI_2$ (0.3 mM C_2BI–$CDPI_2$ in DMSO) and incubated at 23°C for approximately 5 min prior to each fluorescence reading. The fluorescence measurements were conducted at 550 nm excitation and 600 nm emission wavelengths with a slit opening of 5 nm. Under these conditions C_2BI–$CDPI_2$ alone or in the presence of DNA did not interfere with the fluorescence measurements. The absolute binding constant, $K_b = 2.5 \times 10^7$ M^{-1}, was determined from the concentration of agent, 0.1357×10^{-5} M, required for 50% ethidium bromide displacement as measured by a drop in fluorescence to 50% and r = 0.33 was determined from the X-intercept of a plot of % fluorescence versus r.

Thermal DNA denaturation studies

A solution of poly[dA]–poly[dT] (0.798 x 10^{-5} base-pair M) and *seco*-C_2BI–CDPI$_2$ (0.798 x 10^{-6} M) was prepared in 10 mM phosphate buffer (pH = 7.2, 3 mL) to attain a ratio of agent:base pair = 1:10 and the solution was incubated at 23°C for 3 days. The hyperchromicity of the DNA was monitored at 260 nm as a function of temperature. After 3 days the temperature was increased from 23°C to 49°C in increments of 2°C/10 min and from 49°C to 85°C in increments of 3°C/10 min. The absorbance of the solution versus temperature was plotted and the T_m = 75°C (ΔT_m = 22°C) was obtained from the graph. Poly[dA]–poly[dT] exhibited a T_m = 53°C under identical conditions and when the incubation of the DNA–agent solution was conducted for 24 h, 23°C the measured ΔT_m was 9°C (T_m = 62°C).

DNA alkylation and cross-linking studies

Eppendorf tubes containing singly ^{32}P 5'-end-labeled double-stranded DNA prepared exactly as previously detailed[26] (9 μL, in TE buffer) were treated with the agent in a solution of DMSO (1 μL, at the specified concentrations). The reaction was mixed by vortexing and brief centrifugation and subsequently incubated at 37°C for 72 h (C_2BI–CDPI$_2$ agents) or at 4°C for 24 h (CBI–CDPI$_2$ agents). The DNA was separated from unbound agent by EtOH precipitation of the DNA. The EtOH precipitations were carried out by adding t-RNA as a carrier (1, μL, 10 μg/μL), a buffer solution containing salt (0.1 volume, 3M NaOAc in TE) and -20°C EtOH (2.5 volumes). The solutions were mixed and chilled at -70°C in an EtOH dry-ice bath for 30 min. The DNA was reduced to a pellet by centrifugation at 4°C for 15 min, washed with -20°C EtOH (70% in TE containing 0.2 M NaCl), and recentrifuged briefly. The pellets were dried in a Savant Speed Vac concentrator and resuspended in TE buffer (10 μL). The buffer solutions of alkylated DNA were warmed at 100°C for 30 min to induce cleavage at the alkylation sites. After brief centrifugation, formamide dye solution was added (5 μL) to the supernatant. Prior to electrophoresis, the samples were warmed at 100°C for 5 min, placed in an ice bath, and the supernatant (2.4 μL) was loaded onto a gel. Sanger dideoxynucleotide sequencing reactions were run as standards adjacent to the agent DNA reactions. Gel electrophoresis was carried out on a 8% PAGE gel (19:1 acrylamide:*N,N'*-methylenebisacrylamide; 8 M urea). Electrophoresis running buffer (TBE) contained Tris base (100 mM), boric acid (100 mM), and Na_2EDTA–$2H_2O$ (0.2 mM) dissolved in water. PAGE was pre-run for 30 min with formamide dye solution [xylene cyanol FF (0.03%), bromophenol blue (0.03%), and aqueous Na_2EDTA (8.7%, 250 mM)] prior to loading the samples. Autoradiography of dried gels was carried out at -70°C using Kodak X-Omat AR film and a Picker Spectra™ intensifying screen.

The cross-linking reactions were conducted under identical conditions at 37°C, 24 h with the exception that the thermal DNA cleavage step (30 min, 100°C) was omitted and the thermal denaturation time was reduced (100°C, 3 min). Psoralen (10^{-1}, 10^{-2}, and 10^{-3} M) was run as a positive control with cross-linking induced by photochemical irradiation at 365 nm for 1 h.

Acknowledgements

This work was assisted through the financial support of the National Institutes of Health (CA41986 and CA55276) and we wish to thank H. Zarrinmayeh for Figures 5 and 8.

References

1. Chidester, C. G.; Krueger, W. C.; Mizsak, S. A.; Duchamp, D. J.; Martin, D. G. (1981) *J. Am. Chem. Soc.* **103,** 7629. Hanka, L. J.; Dietz, A.; Gerpheide, S. A.; Kuentzel, S. L.; Martin, D. G. (1978) *J. Antibiot.* **31,** 1211.

2. Warpehoski, M. A.; Hurley, L. H. (1988) *Chem. Res. Toxicol.* **1,** 315.

3. Hurley, L. H.; Needham-VanDevanter, D. R. (1986) *Acc. Chem. Res.* **19,** 230.

4. Reynolds, V. L.; McGovren, J. P.; Hurley, L. H. (1986) *J. Antibiot.* **39,** 319.

5. Boger, D. L. in *Advances in Heterocyclic Natural Products Synthesis,* Vol. 2; pp. 1-188; Pearson, W. H., Ed.; JAI press: Greenwich (1992).

6. Coleman, R. S.; Boger, D. L. in *Studies in Natural Products Chemistry,* Vol. 3; p. 301; Atta-ur-Rahman, Ed.; Elsevier: Amsterdam (1989).

7. Boger, D. L. in *Heterocycles in Bioorganic Chemistry;* p. 103; Bergman, J.; Van der Plas, H. C.; Simonyi, M. Eds.; Royal Society of Chemistry: Cambridge (1991).

8. Rawal, V. H.; Jones, R. J.; Cava, M. P. (1987) *Heterocycles* **25,** 701.

9. Ichimura, M.; Muroi, K.; Asano, K.; Kawamoto, I.; Tomita, F.; Morimoto, M.; Nakano, H. (1988) *J. Antibiot.* **41,** 1285. Takahashi, I.; Takahashi, K.; Ichimura, M.; Morimoto, M.; Asano, K.; Kawamoto, I.; Tomita, F.; Nakano, H. (1988) *J. Antibiot.* **41,** 1915.

10. Ohba, K.; Watabe, H.; Sasaki, T.; Takeuchi, Y.; Kodama, Y.; Nakazawa, T.; Yamamoto, H.; Shomura, T.; Sezaki, M.; Konda, S. (1988) *J. Antibiot.* **41,** 1515.

11. Boger, D. L. (1991) *Chemtracts: Org. Chem.* **4,** 329.

12. Boger, D. L., Ishizaki, T.; Zarrinmayeh, H.; Munk, S. A.; Kitos, P. A.; Suntornwat, O. (1990) *J. Am. Chem. Soc.* **112,** 8961.

13. CI-TMI: Boger, D. L.; Ishizaki, T.; Zarrinmayeh, H.; Kitos, P. A.; Suntornwat, O. (1990) *J. Org. Chem.* **55,** 4499. (+)-Duocarmycin SA: Boger, D. L.; Machiya, K. (1992) *J. Am. Chem. Soc.* **114,** 10056. Duocarmycin A: Fukuda, Y.; Nakatani, K.; Terishima, S. (1992) *BioMed. Chem. Lett.* **2,** 759. Fukuda, Y.; Nakatani, K.; Ito, Y.; Terashima, S. (1990) *Tetrahedron Lett.* **31,** 6694.

14. Boger, D. L.; Coleman, R. S. (1988) *J. Am. Chem. Soc.* **110,** 1321, 4796. Boger, D. L.; Coleman, R. S.

(1988) *J. Org. Chem.* **53,** 695. Boger, D. L.; Zarrinmayeh, H. (1990) *J. Org. Chem.* **55,** 1379. Synthesis of the CPI subunit of CC-1065: Wierenga, W. (1981) *J. Am. Chem. Soc.* **103,** 5621. Magnus, P.; Gallagher, T.; Schultz, J.; Or, Y.-S.; Ananthanarayan, T. P. (1987) *J. Am. Chem. Soc.* **109,** 2706. Kraus, G. A.; Yue, S.; Sy, J. (1985) *J. Org. Chem.* **50,** 283. Bolton, R. E.; Moody, C. J.; Pass, M.; Rees, C. W.; Tojo, G. (1988) *J. Chem. Soc., Perkin Trans. 1* 2491. Sundberg, R. J.; Baxter, E. W.; Pitts, W. J.; Ahmed-Schofield, R.; Nishiguchi, T. (1988) *J. Org. Chem.* **53,** 5097. Sundberg, R. J.; Pitts, W. J. (1991) *J. Org. Chem.* **56,** 3048. Toyota, M.; Fukumoto, K. (1992) *J. Chem. Soc., Perkin Trans. 1* 547.

15. Boger, D. L.; Coleman, R. S.; Invergo, B. J.; Sakya, S. M.; Ishizaki, T.; Munk, S. A.; Zarrinmayeh, H.; Kitos, P. A.; Thompson, S. C. (1990) *J. Am. Chem. Soc.* **112,** 4623.

16. Hurley, L. H.; Warpehoski, M. A.; Lee, C.-S.; McGovren, J. P.; Seahill, T. A.; Kelly, R. C.; Mitchell, M. A.; Wicnienski, N. A.; Gebhard, I.; Johnson, P. D.; Bradford, V. S. (1990) *J. Am. Chem. Soc.* **112,** 4633.

17. Warpehoski, M. A.; Gebhard, I.; Kelly, R. C.; Krueger, W. C.; Li, L. H.; McGovren, J. P.; Prairie, M. D.; Wicnienski, N.; Wierenga, W. (1988) *J. Med. Chem.* **31,** 590.

18. CI-based agents: Boger, D. L.; Wysocki, R. J., Jr.; Ishizaki, T. (1990) *J. Am. Chem. Soc.* **112,** 5230. Boger, D. L.; Wysocki, R. J., Jr. (1989) *J. Org. Chem.* **54,** 1238. Boger, D. L.; Ishizaki, T.; Zarrinmayeh, H.; Kitos, P. A.; Suntornwat, O. (1990) *J. Org. Chem.* **55,** 4499. Boger, D. L.; Ishizaki, T.; Zarrinmayeh, H.; Munk, S. A.; Kitos, P. A.; Suntornwat, O. (1990) *J. Am. Chem. Soc.* **112,** 8961. Drost, K. J.; Jones, R. J.; Cava, M. P. (1989) *J. Org. Chem.* **54,** 5985.

19. CBI-based agents: Boger, D. L.; Yun, W.; Teegarden, B. R. (1992) *J. Org. Chem.* **57,** 2873. Boger, D. L.; Ishizaki, T.; Wysocki, R. J., Jr.; Munk, S. A.; Kitos, P. A.; Suntornwat, O. (1989) *J. Am. Chem. Soc.* **111,** 6461. Boger, D. L.; Ishizaki, T. (1990) *Tetrahedron Lett.* **31,** 793. Boger, D. L.; Ishizaki, T.; Kitos, P. A.; Suntornwat, O. (1990) *J. Org. Chem.* **55,** 5823. Boger, D. L.; Ishizaki, T.; Zarrinmayeh, H.; Kitos, P. A.; Suntornwat, O. (1991) *BioMed. Chem. Lett.* **1,** 55. Drost, K. J.; Cava, M. P. (1991) *J. Org. Chem.* **56,** 2240.

20. Boger, D. L.; Ishizaki, T.; Sakya, S. M.; Munk, S. A.; Kitos, P. A.; Jin, Q.; Besterman, J. M. (1991) *BioMed. Chem. Lett.* **1,** 115.

21. CI-based agents: Boger, D. L.; Zarrinmayeh, H.; Munk, S. A.; Kitos, P. A.; Suntornwat, O. (1991) *Proc. Natl Acad. Sci. U.S.A.* **88,** 1431. Boger, D. L.; Munk, S. A.; Zarrinmayeh, H. (1991) *J. Am. Chem. Soc.* **113,** 3980. See also Ref. 26.

22. CBI-based agents: Boger, D. L.; Munk, S. A. (1992) *J. Am. Chem. Soc.* **114,** 5487. Boger, D. L.; Munk, S. A.; Ishizaki, T. (1991) *J. Am. Chem. Soc.* **113,** 2779.

23. Boger, D. L.; Yun, W.; Terashima, S.; Fukuda, Y.; Nakatani, K.; Kitos, P. A.; Jin, Q. (1992) *BioMed. Chem. Lett.* **2,** 759.

24. Boger, D. L.; Palanki, M. S. S. (1992) *J. Am. Chem. Soc.* **114,** 9318.

25. Ambrose, C.; Rajadhyaksha, A.; Lowman, H.; Bina, M. (1989) *J. Mol. Biol.* **210,** 255.

26. Boger, D. L.; Munk, S. A.; Zarrinmayeh, H.; Ishizaki, T.; Haught, J.; Bina, M. (1991) *Tetrahedron* **47,** 2661.

27. Boger, D. L.; Coleman, R. S.; Invergo, B. J.; Zarrinmayeh, H.; Kitos, P. A.; Thompson, S. C.; Leong, T.; McLaughlin, L. W. (1990) *Chem.-Biol. Interactions* **73,** 29.

28. Boger, D. L.; Sakya, S. M. (1992) *J. Org. Chem.* **57,** 1277.

29. Boger, D. L.; Coleman, R. S.; Invergo, B. J. (1987) *J. Org. Chem.* **52,** 1521. Boger, D. L.; Coleman, R. S. (1984) *J. Org. Chem.* **49,** 2240.

30. Baguley, B. C.; Falkenhaug, E.-M. (1978) *Nucl. Acids Res.* **5,** 161.

31. The binding constant measurements were conducted as previously detailed with the exception that the DNA–agent incubation was conducted for 5 min versus 30 min at each point.

32. Sanger, F.; Nicklen, S. Coulsen, A. R. (1977) *Proc. Natl Acad. Sci. U.S.A.* **74,** 5463.

33. Site 1 is the w794 high affinity site modeled in Fig. 3.

34. In addition, the selectivity of the exceptionally weak alkylation by *seco*-C_2BI–TMI appears to closely resemble that of (+)- and (–)-CBI–$CDPI_2$ rather than C_2BI–$CDPI_2$ within w836 DNA.

35. For additional DNA cross-linking agents based on the CC-1065 structure, see: Mitchell, M. A.; Johnson, P. D.; Williams, M. G.; Aristoff, P. A. (1989) *J. Am. Chem. Soc.* **111,** 6428. Mitchell, M. A.; Kelly, R. C.; Wicnienski, N. A.; Hatzenbuhler, N. T.; Williams, M. G.; Petzold, G. L.; Slightom, J. L.; Siemieniak, D. R. (1991) *J. Am. Chem. Soc.* **113,** 8994. Lee, C.-S.; Gibson, N. W. (1991) *Cancer Res.* **51,** 6586.

36. Boger, D. L.; Yasuda, M.; Mitscher, L. A.; Drake, S. D.; Kitos, P. A.; Thompson, S. C. (1987) *J. Med. Chem.* **30,** 1918.